Study of top quark dipole interactions in $t\bar{t}$ production associated with two heavy gauge bosons at the LHC

Seyed Mohsen Etesami, Sara Khatibi, and Mojtaba Mohammadi Najafabadi
School of Particles and Accelerators, Institute for Research in Fundamental Sciences (IPM), P.O. Box 19395-5531, Tehran, Iran

(Received 23 December 2017; published 17 April 2018)

In this paper, we investigate the prospects of measuring the strong and weak dipole moments of the top quark at the Large Hadron Collider (LHC). Measurements of these couplings provide an excellent opportunity to probe new physics interactions as they have quite small magnitudes in the standard model. Our analyses are performed using the production cross sections of $t\bar{t}WW$ and $t\bar{t}ZZ$ processes in the same sign dilepton and four-lepton final states, respectively. The sensitivities to strong and weak top quark dipole interactions at the 95% confidence level for various integrated luminosity scenarios are derived and compared with other studies. To estimate the constraints, the main source of backgrounds and a realistic simulation of the detector response are considered.

DOI: 10.1103/PhysRevD.97.075023

I. INTRODUCTION

The search for new physics beyond the standard model (SM) is one of the main purposes of the CERN Large Hadron Collider (LHC). At the LHC, the impacts of beyond the SM physics could be directly seen, providing that the characteristic scale would be below the center of mass energy of the related hard processes. If not, the new physics effects need to be explored via the accurate measurements of the couplings of the SM particles. According to the recent LHC results, all measurements are found to be in agreement with the SM predictions [1]. This could be a hint that possible new degrees of freedom are separated in mass from the SM fields. As a result, the available energy in the LHC collisions is not enough for direct production of the heavy degrees of freedom coming from beyond the SM. Therefore, one could parametrize the effects of all new physics by a series of $SU(3)_c \times SU(2)_L \times U(1)_Y$ gauge invariant operators $\mathcal{O}_i$ constructed out of the SM fields [2–5]. These operators should be of dimension $d > 4$ and typically the leading effects for collider observables show up at $d = 6$. Their coefficients are suppressed by inverse powers of the scale of new physics Λ:

$$\mathcal{L}_{\text{eff}} = \mathcal{L}_{\text{SM}} + \sum_i \frac{c_i \mathcal{O}_i^{(6)}}{\Lambda^2}, \tag{1}$$

where $\mathcal{L}_{\text{SM}}$ denotes the SM Lagrangian and c_i are the dimensionless Wilson coefficients. Such a *model independent* parametrization has the possibility to be linked to the ultraviolet completions and the results could be interpreted in various beyond the SM theories. The dimension six operators $\mathcal{O}_i^{(6)}$ have been listed in Refs. [2–4]. Studies on the validity of the SM effective field theory (EFT) and the fact that the EFT validity range could not be obtained only on the basis of low energy information is available in Ref. [6].

From the theoretical point of view, the top quark could provide a unique way into beyond the SM physics, since the top quark Yukawa coupling is the largest among all other SM fermions. Particularly, the CP properties of top quark interactions with the SM fields is one of the important subjects to study in the top quark sector [7]. Especially, it has been shown that the CP-violating couplings of the top quark in the framework of a model with an extended scalar sector can explain the observed baryon asymmetry of the universe [8]. In the top quark sector, within a beyond SM theory, CP-violating interactions may also show up through the form of electric, strong, and weak dipole moments. So far, there have been many studies of the potential for revealing possible effects of new physics in the top quark sector at the LHC, Tevatron and future colliders using the higher-dimensional operators [9–61].

With the LHC phase II upgrade, in which a large amount of data is going to be collected and several experimental efforts are going on to assess and reduce the systematic uncertainties, rare SM processes will become accessible [62–64]. In particular, final states containing several heavy SM degrees of freedom could be observed and new physics

effects can be studied through them as they have a small amount of backgrounds. For instance, $pp \to t\bar{t}VV$ processes, where $V = Z$, $W^{\pm}$ are of the promising channels through which new physics beyond the SM can be investigated. Studying these processes has the advantage of having naturally high multiplicity final states and consequently the backgrounds are better under control. Large thresholds of $2(m_t + m_V)$ with $V = W$, Z for $t\bar{t}WW$ and $t\bar{t}ZZ$ productions, restricts the phase space and lead to small production cross sections at the level of few femtobarns. However, LHC is able to reach the threshold and its experiments are able to observe these processes as around 78 $t\bar{t}ZZ$ and 435 $t\bar{t}WW$ events are expected to be produced per 30 fb^{-1} of integrated luminosity of data. It is worth mentioning that so far the ATLAS and CMS experiments have measured the top pair production cross sections in association with a single W or Z boson [65,66]. Measuring the $t\bar{t}WW$ and $t\bar{t}ZZ$ rates at the LHC is in particular remarkable in top quark sector as they provide the possibility to probe the top quark couplings with the SM heavy gauge bosons and even multigauge boson interactions. This allows direct probes for dynamics of electroweak symmetry breaking.

In this paper, our concentration is especially on studying the strong and weak electric and magnetic dipole moments of the top quark through the $pp \to t\bar{t}WW$ and $pp \to t\bar{t}ZZ$ processes at the LHC. In the SM framework at tree level, the magnetic and electric dipole moments are zero and they could be generated at higher order electroweak corrections which have small magnitudes [67]. However, sizable enhancements are predicted in the various extensions of the SM [32,67]. Therefore, observation of these moments with deviations from the SM predictions would be indicative of beyond the SM physics. A highly motivated task would be to investigate how precise these dipole moments can be measured at the collider experiments.

The plan of this paper is as follows. In Sec. II, the top quark strong and weak dipole moments are defined in the context of the SM effective field theory and the relations of the dipole moments with the dimension-six operators are given. Section III is dedicated to estimate the sensitivity of the $pp \to t\bar{t}WW$ and $pp \to t\bar{t}ZZ$ processes to the top quark dipole moments and prospects arising from the production rates. The conclusions and results are summarized in Sec. IV.

II. TOP QUARK EFFECTIVE COUPLINGS

As we have mentioned in the previous section, within the SM effective framework, the effects of new physics can be parametrized by using higher-dimensional operators involving the SM fields, assuming these operators come from new degrees of freedom occurring at a large energy scale Λ. Considering dimension-six operators and following Ref. [3], we present the general expressions for the gluon-top-antitop ($gt\bar{t}$) and Z-top-antitop ($Zt\bar{t}$) vertices here.

A. $gt\bar{t}$ vertex

The most general $gt\bar{t}$ coupling considering dimension-six operators, including the SM part could be parametrized as follows [3]:

$$\mathcal{L}_{gt\bar{t}} = -g_s \bar{t}\frac{\lambda^a}{2}\gamma^\mu t G^a_\mu - g_s \bar{t}\frac{\lambda^a}{2}\frac{i\sigma^{\mu\nu}}{m_t}(d_V^g + i d_A^g \gamma_5) t G^a_{\mu\nu}, \quad (2)$$

where g_s denotes the strong interaction coupling, d_V^g and d_A^g are real parameters which are related to the top quark chromomagnetic and chromoelectric dipole moments, respectively. Gell-Mann matrices are denoted by λ^a and $G^a_{\mu\nu}$ is the strong field strength tensor. At leading-order, in the SM context, d_V^g and d_A^g are zero. The first term in Eq. (2) is the SM interaction, second and third terms which consist of both $gt\bar{t}$ interaction and four-leg $ggt\bar{t}$ coupling come from the dimension six operator [3]:

$$O^{33}_{uG\phi} \sim (\bar{q}_{L3}\lambda_a \sigma^{\mu\nu} t_R)\tilde{\phi} G^a_{\mu\nu}, \quad (3)$$

where $\tilde{\phi} = i\tau_2\phi^*$ and ϕ is the weak doublet of Higgs boson field, q_{L3} is the quark weak doublet of left-handed quark and the right-handed top quark field is denoted by t_R. The imaginery (real) part of $C^{33}_{uG\phi}$ is connected to the chromoelectric (chromomagnetic) dipole moment d_A^g (d_V^g) through the following relations [3]:

$$\delta d_V^g = \frac{\sqrt{2}}{g_s}\mathrm{Re}C^{33}_{uG\phi}\frac{v m_t}{\Lambda^2}, \qquad \delta d_A^g = \frac{\sqrt{2}}{g_s}\mathrm{Im}C^{33}_{uG\phi}\frac{v m_t}{\Lambda^2}, \quad (4)$$

where v is the vacuum expectation value and is equal to 246 GeV. It is notable that no corrections from dimension-six operators are received by the γ_μ term in the Eq. (2). In this study, we consider both chromoelectric and chromomagnetic dipole moments.

In the SM context, the one-loop level QCD corrections can generate d_V^g through the exchange of gluons in two different Feynman diagrams. One of the diagrams is the same as QED case, replacing photon by gluon. Another diagram consists of an external gluon interacting with the internal gluons coming from the non-Abelian nature of QCD. The same as QED case, these diagrams generate nonzero d_V^g which is proportional to α_s/π [67]. It is worth indicating that in addition to QCD corrections, Z and Higgs bosons exchange also generate d_V^g. Including all SM contributions at one-loop, the value of d_V^g is equal to -7×10^{-2} and nonzero value for d_A^g arises from contributions from beyond one-loop and is quite small [67,68].

At present, there are both *direct* and *indirect* bounds on the chromomagnetic and chromoelectric dipole moments of the top quark. The bound could be obtained from the

inclusive and differential top quark pair cross section measurements at the LHC and Tevatron. In Ref. [20], the authors have shown that in particular the presence of top quark chromoelectric dipole moment increases the gluon-gluon fusion process contribution in $t\bar{t}$ production at the Tevatron and LHC. Bounds are derived on both top quark chromoelectric and chromomagnetic dipole moments using the measured ratio $\sigma(gg \to t\bar{t})/\sigma(pp \to t\bar{t})$ and $t\bar{t}$ mass spectrum at the Tevatron [20].

The top pair events produced at the large invariant masses in proton-proton collisions at the center-of-mass energies of 13, 14, and 100 TeV in the semi-leptonic channel have been studied to probe the top quark dipole moments in Ref. [9]. It has been shown that in the boosted regime the QCD background can be considerably suppressed and stringent bounds are achievable. The CMS collaboration has derived limits on these dipole moments from the measured top pair spin correlation at the LHC at 8 TeV [69].

The single top quark production in association with a W boson (tW-channel) is shown to be also a sensitive process to the top quark dipole moments [11,19]. Constraints have been obtained using the measured cross section of tW-channel at the LHC with the center-of-mass energy of 7 TeV using an integrated luminosity of 4.9 fb^{-1}.

Amongst all searches, the strongest limits on d_V^g and d_A^g come from low energy probes like the neutron electric dipole moment (d_n) [70] and the rare decays of B mesons [67]. The constraint on the top quark chromoelectric dipole moment from d_n is found to be: $|d_A^g| \leq 0.95 \times 10^{-3}$ at 90% confidence level (CL) [9]. The measured branching fraction of $b \to s\gamma$ leads to the limits of $-3.8 \times 10^{-3} \leq d_V^g \leq 1.2 \times 10^{-3}$ at the 95% CL [9].

B. $Zt\bar{t}$ vertex

The effective $Zt\bar{t}$ vertex considering the SM contributions and the ones come from dimension six operators can be written as [3]:

$$\mathcal{L}_{Zt\bar{t}} = -\frac{g}{2c_W}\bar{t}\gamma_\mu(X_L P_L + X_R P_R - 2s_W^2 Q_t)tZ^\mu - \frac{g}{2c_W}\bar{t}\frac{i\sigma_{\mu\nu}q^\nu}{m_Z}(d_V^Z + id_A^Z\gamma_5)tZ_\mu, \quad (5)$$

where m_Z and Q_t are the Z boson mass and the top quark electric charge, respectively. In the SM at tree level, $X_L = 1$, $X_R = 0$, and $d_V^Z = d_A^Z = 0$. The contributions to these $Zt\bar{t}$ coupling from the dimension six operators are

$$\delta d_A^Z = \sqrt{2} \times \mathrm{Im}[c_W C_{uW}^{33} - s_W C_{uB\phi}^{33}]\frac{v^2}{\Lambda^2},$$
$$\delta d_V^Z = \sqrt{2} \times \mathrm{Re}[c_W C_{uW}^{33} - s_W C_{uB\phi}^{33}]\frac{v^2}{\Lambda^2}. \quad (6)$$

The contributions of dimension six operators to X_L and X_R are neglected in this analysis [3]. The constraints on d_A^Z and d_V^Z could be translated into limits on the combination of the effective operators. The couplings d_A^Z and d_V^Z are the weak electric and magnetic dipole moments. The weak electric dipole moment coupling is a CP violating coupling which appears at three-loops in the SM and the coupling d_V^Z corresponds to the weak magnetic dipole moment and it is at the order of 10^{-4} in the SM framework [71–74].

There are studies on d_A^Z and d_V^Z at the electron-positron colliders and at the LHC [27,75] to constrain these couplings. In Ref. [75], the potential of a future e^-e^+ collider for examining the electroweak top quark couplings has been presented. Also, they have used the LEP1 data at Z-pole and the electroweak precision data to probe the top quark electroweak couplings.

The top quark weak electric and magnetic dipole moments have been investigated at the LHC and the ILC from the $t\bar{t}Z$ production [27]. Both weak dipole moments are expected to be constrained to ± 0.15 using 300 fb^{-1} of data and would be improved to ± 0.08 with 3 ab^{-1} integrated luminosity of the data. Bounds at the same order can be obtained using the LEP electroweak precision data. The ILC with 500 fb^{-1} is expected to reach the limits of ± 0.08 on the weak electric dipole moment and $[-0.02, 0.04]$ on the weak magnetic dipole moment [27]. It has been shown in Ref. [25] that d_V^Z and d_A^Z can be well probed by the ratio of the cross section of $t\bar{t}Z$ to $t\bar{t}$, because it allows to reduce several sources of the systematic uncertainties considerably.

III. LHC CONSTRAINTS FROM $t\bar{t}VV$

The $pp \to t\bar{t}WW$ and $pp \to t\bar{t}ZZ$ processes are interesting to study because of their small production cross sections in the SM [62] and the significant enhancement that could show up in their rates in several new physics scenarios. In this section, we examine the sensitivity of these processes to the strong and weak top quark electric and magnetic dipole moments at the 14 TeV LHC.

The SM $t\bar{t}WW$ and $t\bar{t}ZZ$ processes produce an interesting set of the final states from which most of them giving rise to important signatures at the LHC. For $t\bar{t}WW$ ($t\bar{t}ZZ$) process, depending on the top quarks and W (Z) bosons decays between zero to four (six) charged lepton(s) might be produced. Lists of $t\bar{t}WW$ and $t\bar{t}ZZ$ decay modes, with at least a charged lepton in the final state, and the related branching fractions are presented in Table I and Table II, respectively.

For the $t\bar{t}WW$ process, the main decay channel is the monoleptonic decay mode which has a branching fraction of 40%, followed by the dilepton, opposite-sign and same-sign (OS + SS) mode with branching fraction of 29.6%. The branching fractions of trilepton and four-lepton decay modes are 9.6% and 1.2%, respectively. Among all the

TABLE I. $t\bar{t}WW$ decay modes where at least a charged lepton in the final state is present.

$t\bar{t}$ decays	WW decays	Channel	Branching fraction%
$(l\nu b)(q\bar{q}'b)$	$(q\bar{q}')(q\bar{q}')$	mono-lepton	20
$(l\nu b)(q\bar{q}'b)$	$(l\nu)(q\bar{q}')$	dilepton (OS + SS)	20
$(l\nu b)(q\bar{q}'b)$	$(l\nu)(l\nu)$	trilepton	4.8
$(l\nu b)(l\nu b)$	$(q\bar{q}')(q\bar{q}')$	dilepton(OS)	4.8
$(l\nu b)(l\nu b)$	$(l\nu)(q\bar{q}')$	trilepton	4.8
$(l\nu b)(l\nu b)$	$(l\nu)(l\nu)$	four-lepton	1.2
$(q\bar{q}'b)(q\bar{q}'b)$	$(l\nu)(l\nu)$	dilepton(OS)	4.8
$(q\bar{q}'b)(q\bar{q}'b)$	$(l\nu)(q\bar{q}')$	mono-lepton	20

TABLE II. $t\bar{t}ZZ$ decay modes where at least a charged lepton in the final state is present.

$t\bar{t}$ decays	ZZ decays	Channel	Branching fraction
$(l\nu b)(q\bar{q}'b)$	$(q\bar{q})(q\bar{q})$	mono-lepton	21
$(l\nu b)(q\bar{q}'b)$	$(\nu\bar{\nu})(\nu\bar{\nu})$	mono-lepton	1.76
$(l\nu b)(q\bar{q}'b)$	$(l^+l^-)(q\bar{q})$	trilepton	6
$(l\nu b)(q\bar{q}'b)$	$(l^+l^-)(l^+l^-)$	five-lepton	0.43
$(l\nu b)(q\bar{q}'b)$	$(l^+l^-)(\nu\bar{\nu})$	trilepton	1.75
$(l\nu b)(q\bar{q}'b)$	$(q\bar{q})(\nu\bar{\nu})$	mono-lepton	12.2
$(l\nu b)(l\nu b)$	$(q\bar{q})(q\bar{q})$	dilepton(OS)	5.18
$(l\nu b)(l\nu b)$	$(\nu\bar{\nu})(\nu\bar{\nu})$	dilepton(OS)	0.43
$(l\nu b)(l\nu b)$	$(l^+l^-)(q\bar{q})$	four-lepton	1.48
$(l\nu b)(l\nu b)$	$(l^+l^-)(l^+l^-)$	six-lepton	0.1
$(l\nu b)(l\nu b)$	$(q\bar{q})(\nu\bar{\nu})$	dilepton	3
$(l\nu b)(l\nu b)$	$(l^+l^-)(\nu\bar{\nu})$	four-lepton	0.43
$(q\bar{q}'b)(q\bar{q}'b)$	$(l^+l^-)(q\bar{q}')$	dilepton(OS)	6.1
$(q\bar{q}'b)(q\bar{q}'b)$	$(l^+l^-)(\nu\bar{\nu})$	dilepton(OS)	1.7
$(q\bar{q}'b)(q\bar{q}'b)$	$(l^+l^-)(l^+l^-)$	four-lepton	0.44

above decay modes the monoleptonic suffers from large background contributions. The channels in particular containing at least a pair of SS charged leptons seem to be the promising search channels for the $t\bar{t}WW$ process. For the $t\bar{t}ZZ$ process, in addition to monolepton, dilepton, trilepton, and four-lepton channels five and six lepton multiplicities are among the possible decay channels. Although the topologies with high lepton multiplicities have small branching fractions, the contributing backgrounds for such cases are quite negligible.

In order to study the sensitivity of the $t\bar{t}WW$ and $t\bar{t}ZZ$ processes to the top quark strong and weak dipole moments, we employ MadGraph5_aMC@NLO package [76] which automatically generates the necessary code for computing the cross section and other observables for the related process. The results are computed using the NNPDF3 PDF sets [77]. The top quark mass is set to 172.5 GeV and the mass of W boson is taken as 80.37 GeV. The calculations are performed at the LHC with the center-of-mass energy of 14 TeV.

To perform the calculations of the cross sections in the presence of the top quark strong and weak dipole moments, the effective Lagrangians are implemented into FeynRules program [78]. Then the effective model is exported into a UFO module [79] which is connected to MadGraph5_aMC@NLO. MadSpin is used for decaying top quarks, W and Z bosons. Pythia 8 [80] is used for parton showering and hadronization. Jets are reconstructed using the anti-k_t algorithm with a radius size of 0.4 [81]. Delphes 3.3.2 [82] is utilized to simulate the response of a CMS-like detector [83] which includes the magnetic field, the calorimeters and all subdetector effects.

A. Top pair production in association with two charged gauge bosons $W^{\pm}W^{\mp}$

In the SM, the production of top quark pair associated with $W^{\pm}W^{\mp}$ comes from either gluon-gluon fusion or quark-anti-quark annihilation. The main contributions are of order $\mathcal{O}(\alpha_s^2\alpha^2)$ and a partonic center-of-mass energy of at least $2m_t + 2m_W$ is necessary which causes a small production cross section at the LHC. Gluon and quark initiated representative Feynman diagrams at leading order contributing to $t\bar{t}WW$ production in the SM are depicted in Fig. 1. In our study the production of $t\bar{t}WW$ is calculated in four flavor scheme (4FS) as in the 5FS case there exists intermediate top quark resonances that must be subtracted [62,84]. It is to avoid of unnecessary complication in calculation of the production rate.

The $t\bar{t}WW$ production cross section at the center-of-mass energy of 14 TeV is calculated using MadGraph5_aMC@NLO package. The next-to-leading order cross section is found to be $14.5\ \text{fb} \pm 3\%\ (\text{PDF})^{+12.3\%}_{-13.0\%}$ (scales). The NLO QCD effects are on the order of 10%. Complete details of the QCD NLO calculations can be found in Refs. [84]. We note that at the 14 TeV LHC, around 54% of the total cross section comes from the gluon-gluon fusion which goes higher at the larger center-of-mass energies because of growing the gluon PDF.

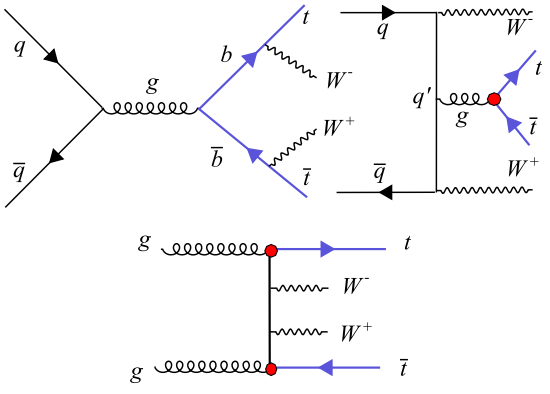

FIG. 1. Lowers-order representative Feynman diagrams for $t\bar{t}WW$ production at the LHC. The vertices which receive contribution from $O^{33}_{uG\phi}$ operator are shown with red filled circles.

The LO contributions of the top quark chromoelectric (d_A^g) and chromomagnetic (d_V^g) dipole moments, arising from $O_{uG\phi}^{33}$ operator, to the $t\bar{t}WW$ rate is calculated with MADGRAPH5_AMC@NLO. The relative corrections from d_A^g and d_V^g to the total cross section of $\sigma(pp \to t\bar{t}WW)$ has the following form:

$$\frac{\Delta\sigma(pp \to t\bar{t}WW)}{\sigma_{\rm SM}} = \alpha_i d_i^g + \beta_i (d_i^g)^2, \qquad i = V, A, \tag{7}$$

where $\sigma_{\rm SM}$ is the SM cross section and α_i is the interference term which its contribution is of the order of Λ^{-2}. The β_i terms correspond to the pure $O_{uG\phi}^{33}$ contributions which has the power of Λ^{-4}. Without taking into account the dimension eight operators, such terms could be dropped because dimension eight operators generate contributions at similar order. However, we keep Λ^{-4} term as it is the first appearing term in the cross section for d_A^g and it is relevant to have it when obtaining constraints on d_V^g. Of course, it is expected that the cross section has a symmetric shape around $d_A^g = 0$ as it is a CP even observable leading to $\alpha_A = 0$. To extract the coefficients α_i and β_i in Eq. (7), the calculations with d_A^g and d_V^g are performed assuming different values: 0.0, ±01, ±0.2, ±0.3 and fit the obtained cross sections to Eq. (7). The coefficients α_i and β_i are presented in Table III.

To derive a quantitative estimate of the constraints that could be optimistically reached under various integrated luminosity scenarios, we concentrate on the exactly two same sign charged lepton (e, μ) topology. To select the same sign dilepton events, we require to have exactly two SS leptons with transverse momentum greater than 25 GeV and $|\eta_l| < 2.5$. The angular separation of the leptons, $\Delta R(l_1, l_2) = \sqrt{(\Delta\eta)^2 + (\Delta\phi)^2}$, is requested to larger than 0.4. The event is required to contain at least four jets from which at least two have to be b-tagged jets. The jets are required to have transverse momentum greater than 25 GeV within the pseudorapidity range of $|\eta| < 2.5$. A cut of 40 GeV is applied on the missing transverse energy.

We continue to set an upper limit on the $t\bar{t}WW$ production cross section in the presence of strong chromoelectric or chromomagnetic dipole moments. To derive constraints on d_V^g and d_A^g, a counting experiment technique is employed. The method is to begin with a Poisson distribution describing the probability for measuring N events:

TABLE III. Values of α_i and β_i for the 14 TeV LHC.

i	α_i	β_i
V	−1.2	1783.5
A	0.0	1950.8

$$\mathcal{P}(N|\sigma_{t\bar{t}WW} \times \epsilon \times \mathcal{L}, B) = e^{-(\sigma_{t\bar{t}WW} \times \epsilon \times \mathcal{L} + B)} \times \frac{(\sigma_{t\bar{t}WW} \times \epsilon \times \mathcal{L} + B)^N}{N!}, \tag{8}$$

where $\sigma_{t\bar{t}WW}$, $\mathcal{L}$, ϵ and B are the signal cross section in the presence of d_V^g and d_A^g, the integrated luminosity, the efficiency of signal after the selection criteria, and the expected background events corresponding to the assumed integrated luminosity. At 95% confidence level (CL), the upper limit on the signal cross section can be calculated with integration over the posterior probability according to the following:

$$0.95 = \frac{\int_0^{\sigma^{95\%}} \mathcal{P}(N|\sigma_{t\bar{t}WW} \times \epsilon \times \mathcal{L}, B)}{\int_0^{\infty} \mathcal{P}(N|\sigma_{t\bar{t}WW} \times \epsilon \times \mathcal{L}, B)}. \tag{9}$$

In this exploratory study, the number of background events is obtained as $B = (\sigma_{t\bar{t}WW}^{\rm SM} + \sigma_{t\bar{t}W}^{\rm SM}) \times \mathcal{L}$ where $\sigma_{t\bar{t}WW}^{\rm SM}$ and $\sigma_{t\bar{t}W}^{\rm SM}$ are the SM production rate for $t\bar{t}WW$ and $t\bar{t}W$ processes after the selection cuts described above. To be more realistic, the SM production cross section of these backgrounds are scaled to their NLO value. The efficiency ϵ after the selection is found to be 22.6% where a realistic experimental simulation which considers detector response is considered.

We obtain the expected upper limit at the 95% CL on the signal cross section and compare it with the theoretical signal cross section to find the upper limits on d_V^g and d_A^g. The resulting limits are calculated for three scenarios of integrated luminosities of 30, 300, 3000 fb^{-1} and presented in Table IV. For example, with an integrated luminosity of 30 fb^{-1} the upper limits of $-0.036 \le d_V^g \le 0.037$ and $|d_A^g| \le 0.035$ are derived. If we assume 10% uncertainty on the signal efficiency and 100% uncertainty on the number of background events, the bounds on d_V^g and d_A^g at 30 fb^{-1} are loosen to $-0.043 \le d_V^g \le 0.044$ and $|d_A^g| \le 0.042$.

We note that including the other signatures of $t\bar{t}WW$ process such as trilepton and four lepton would increase the sensitivity of this channel to the strong electric and magnetic dipole moments of the top quark. In the end of this section, it should be indicated that in addition to $gt\bar{t}$ effective couplings, $t\bar{t}WW$ process is sensitive to the anomalous Wtb and $Zt\bar{t}$ vertices. The effective Lagrangian up to dimension six operators explaining the anomalous Wtb coupling as follows [3]:

TABLE IV. Limits on d_V^g and d_A^g at 95% CL corresponding to 30, 300, and 3000 fb^{-1} integrated luminosities obtained from $t\bar{t}WW$ process.

Coupling	30 fb^{-1}	300 fb^{-1}	3000 fb^{-1}
d_V^g	[−0.036, 0.037]	[−0.020, 0.021]	[−0.011, 0.012]
d_A^g	[−0.035, 0.035]	[−0.019, 0.019]	[−0.011, 0.011]

$$\mathcal{L}_{\mathrm{Wtb}} = -\frac{g}{\sqrt{2}}\bar{b}\Big(\gamma^{\mu}(V_L P_L + V_R P_R) + \frac{i\sigma_{\mu\nu}q^{\nu}}{m_W}(g_L P_L + g_R P_R)\Big)tW_{\mu}^{-} + \mathrm{H.c.}, \quad (10)$$

where $V_{L,R}$ and $g_{L,R}$ are dimensionless couplings. At tree level within the SM, $V_L = V_{tb}$ and $V_R = g_L = g_R = 0$. From the rare B-meson decay, the constraints on these couplings are found to be [85]:

$$-0.0007 < V_R < 0.0025, \qquad -0.0013 < g_L < 0.0004,$$
$$-0.15 < g_R < 0.57. \quad (11)$$

The 95% CL bounds derived from W boson polarization and measured cross section of the single top t-channel at the LHC are [86]: $-0.13 < V_R < 0.18$, $-0.09 < g_L < 0.06$, and $-0.15 < g_R < 0.01$. The total cross section of $t\bar{t}WW$ process does not show considerable sensitivity to g_L and g_R. By setting $g_R = 0.1$ and $g_L = 0.1$, the relative change of $t\bar{t}WW$ rate is 4% and 0.24%, respectively. This means that no strong limits on g_L and g_R are expected to be obtained from $t\bar{t}WW$ channel.[1]

We also note that in $t\bar{t}WW$ production, there are diagrams containing $Zt\bar{t}$ vertex resulting to the fact that the weak dipole moments d_V^Z and d_A^Z contribute to $t\bar{t}WW$ cross section. We do not consider this in our analysis as the modification to $\sigma(pp \to t\bar{t}WW)$ due to $d_{V,A}^Z$ is found to be at the level of less than 10% when these couplings vary up to the value of ± 0.05.

B. Top pair production in association with two neutral heavy gauge bosons ZZ

In this section, we study the sensitivity of the $t\bar{t}ZZ$ production to the top quark dipole moments. The representative Feynman diagrams at leading order of this process are depicted in Fig. 2. The next-to-leading-order cross section of $t\bar{t}ZZ$ process is calculated using MadGraph5_aMC@NLO is found to be: 2.6 fb $\pm$ 1.82% (PDF)$^{+4.34\%}_{-8.78\%}$ (scales), where the first uncertainty gives the contribution from the dependence on the choice of parton distribution functions and the second part is the factorization and renormalization scale uncertainties [62,84]. The input parameters for the cross section calculation has been taken similar to the previous section. The NLO corrections to the $t\bar{t}ZZ$ production is quite small resulting to a k-factor close to one [84]. The leading order cross section is proportional to $\mathcal{O}(\alpha_s^2\alpha^2)$ and a partonic center-of-mass energy of at least $2m_t + 2m_Z$ is necessary for such a final state at the LHC. The presence of α^2 and four heavy particles in the final state, which causes to reduce the phase space, lead to such a small rate for this process.

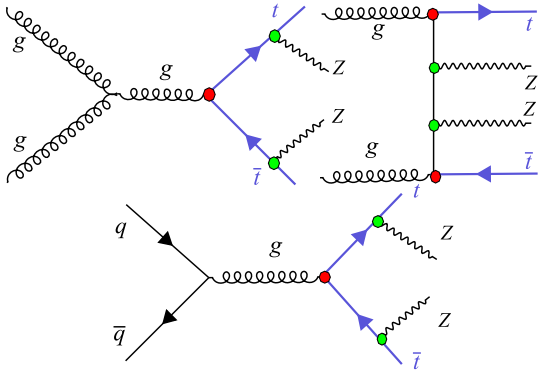

FIG. 2. Representative Feynman diagrams for $t\bar{t}ZZ$ production at leading-order.

The $t\bar{t}ZZ$ channel allows us to probe both the strong ($d_{V,A}^g$) and weak ($d_{V,A}^Z$) top quark dipole moments. The contributions of the strong and weak dipole moments to the $t\bar{t}ZZ$ productions cross section is calculated using MadGraph5_aMC@NLO package. The relative modifications from operators $O_{uG\phi}^{33}$, O_{uW}^{33} and $O_{uB\phi}^{33}$ to the total cross section of $\sigma(pp \to t\bar{t}ZZ)$ in terms of $d_{V,A}^g$ and $d_{V,A}^Z$ can be written as:

$$\frac{\Delta\sigma(pp \to t\bar{t}ZZ)}{\sigma_{\mathrm{SM}}} = \rho_i^{g,Z} d_i^{g,Z} + \gamma_i^{g,Z}(d_i^{g,Z})^2, \quad i = V,A, \quad (12)$$

where $\rho_i^{g,Z}$ term is the interference term of the SM with new physics which is of the order of Λ^{-2}. The $\gamma_i^{g,Z}$ term is corresponding to the pure $O_{uG\phi}^{33}$, O_{uW}^{33} and $O_{uB\phi}^{33}$ contributions appearing with the power of Λ^{-4}. To obtain the coefficients $\rho_i^{g,Z}$ and $\gamma_i^{g,Z}$ in Eq. (12), the cross sections are calculated in the presence of these coefficients taking various values: 0.0, $\pm$01, $\pm$0.2, $\pm$0.3, then the results are fitted to Eq. (12). The coefficients $\rho_i^{g,Z}$ and $\gamma_i^{g,Z}$ are given in Table V. We see the interference term coefficient (for $i = V$) is small and the pure new physics coefficients are almost close to each other. As expected due to the presence of q_μ factor in the effective Lagrangian, the coefficients $\gamma_{V,A}^{g,Z}$ are very large.

As mentioned before, there are several signatures for $t\bar{t}ZZ$ that all contain at least two b-jets which come from the weak top quark decay. Among all signatures, we take the four-lepton (lepton $= e$, μ) final state which is a clean signature. Requiring four leptons and two b-tagged jets in

TABLE V. Values of $\rho_i^{g,Z}$ and $\gamma_i^{g,Z}$ for the 14 TeV LHC.

i	ρ_i^g	γ_i^g	ρ_i^Z	γ_i^Z
V	−6.0	2127.2	0.1	27.5
A	0.0	2092.4	0.0	27.8

[1]The correct prediction for examining the sensitivity of the $t\bar{t}WW$ process to the anomalous Wtb should be performed by including the top quark decays since two additional Wtb vertices appear.

TABLE VI. Limits on $d_V^{g,Z}$ and $d_A^{g,Z}$ at 95% CL corresponding to 30, 300, and 3000 fb^{-1} integrated luminosities obtained from $t\bar{t}ZZ$ process.

Coupling	30 fb^{-1}	300 fb^{-1}	3000 fb^{-1}
d_V^g	[−0.036, 0.039]	[−0.019, 0.022]	[−0.010, 0.012]
d_A^g	[−0.037, 0.037]	[−0.020, 0.020]	[−0.011, 0.011]
d_V^Z	[−0.32, 0.33]	[−0.18, 0.17]	[−0.10, 0.09]
d_A^Z	[−0.32, 0.21]	[−0.18, 0.18]	[−0.10, 0.10]

the final state should be enough to increase the signal-to-background ratio significantly. To select the signal events, we require to have exactly four leptons with $p_T > 25$ GeV and $|\eta| < 2.5$. The missing transverse energy has to be larger than 40 GeV and each event is requested to contain at least two b-tagged jets. The jets are required to have $p_T > 25$ GeV and $|\eta| < 2.5$. To have well isolated objects in the final state, it is required $\Delta R(l_i, l_j) > 0.4$, $\Delta R(j_i, j_j) > 0.4$, and $\Delta R(l_i, j_j) > 0.4$.

We follow the same method as described in the previous section to set upper limit on the signal cross section then the upper limit is translated into the limits on the top quark dipole moments. The SM $t\bar{t}ZZ$ and $t\bar{t}Z$ are taken as the main backgrounds and the number of background events is obtained through $B = (\sigma_{t\bar{t}ZZ}^{\rm SM} + \sigma_{t\bar{t}Z}^{\rm SM}) \times \mathcal{L}$ where $\sigma_{t\bar{t}ZZ}^{\rm SM}$ and $\sigma_{t\bar{t}Z}^{\rm SM}$ are the SM rates after the selection cuts described above. After the described selection, the efficiency ϵ is obtained to be equal to 19.4%. The bounds on $d_{V,A}^g$ and $d_{V,A}^Z$ are shown in Table VI for 30, 300 and 3000 fb^{-1} integrated luminosity of data.

Assuming a 10% overall uncertainty on the efficiency of signal and 100% uncertainty on the number of background events make limits looser. Using 30 fb^{-1} integrated luminosity of data, the bounds on d_V^g and d_A^g become $-0.043 \leq d_V^g \leq 0.045$ and $|d_A^g| \leq 0.044$.

One can derive a lower limit on the new physics characteristic scale using the Eq. (4) and taking the Wilson coefficient $C_{uG\phi}^{33}$ to be at most equal to 4π. Using for instance the obtained upper limit on d_V^g at 3000 fb^{-1}, a lower bound of $\Lambda \sim 9$ TeV is deduced. Of course, choosing lower value of $C_{uG\phi}^{33}$ leads to looser limit on Λ.

C. Comparison of the results with other studies

In this section, we compare the sensitivity of the expected constraints from the $t\bar{t}WW$ (same-sign leptons) analysis and $t\bar{t}ZZ$ (four-lepton) analysis with some other studies. The results of this study with two scenarios of integrated luminosities 300 and 3000 fb^{-1} are compared with others in Fig. 3. The most stringent direct bounds from the FCC-hh, where protons are collided with $\sqrt{s} = 100$ TeV, are based on the integrated luminosity of 10 ab^{-1} [9] and are derived from the events with central jets ($|\eta| < 2$) and transverse momentum larger than 1 TeV reconstructed using an anti-k_T [81] algorithm with a radius size of 0.2. The FCC-hh limits are obtained in an optimal invariant mass region of the top quark pair mass of $m_{t\bar{t}} > 10$ TeV.

The indirect limits on d_V^g are based on rare B meson decay [67] which has been found to be $-0.0038 \leq d_V^g \leq 0.0012$. In particular, the upper limit is the most stringent one which is even stronger than the expected bound from FCC-hh. The combination of the measured top quark pair cross section at the LHC8 and Tevatron lead to $-0.012 \leq d_V^g \leq 0.023$ [9] and the expected limit derived from the $t\bar{t}$ spectrum and the inclusive cross section at the LHC14 based on 100 fb^{-1} is $-0.0086 \leq d_V^g \leq 0.012$ [9]. The limits from our analyses are comparable to these limits and could be even improved if the other signatures presented in Table I and Table II are taken into account.

For the d_A^g case, the indirect limits have been extracted from the upper limit on the neutron electric dipole moment. This indirect low energy limit which is $|d_A^g| \leq 0.00095$ [70] is the strongest one. Again, among the direct limits, the one obtained from FCC-hh is the most stringent limit: $|d_A^g| \leq 0.0026$. The combination of the measured $t\bar{t}$ cross section at the LHC8 and Tevatron implies $|d_A^g| \leq 0.087$ [9]

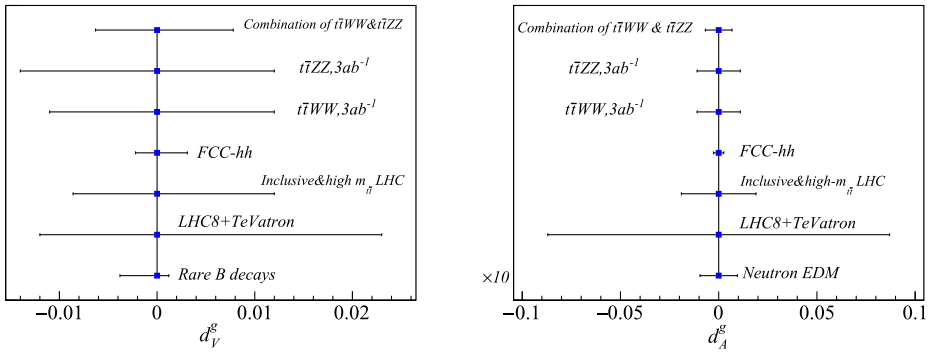

FIG. 3. The limits at 95% CL on d_V^g (right panel) and on d_A^g (left panel) from $t\bar{t}WW$ (same-sign leptons) and $t\bar{t}ZZ$ (four-lepton) with 300 and 3000 fb^{-1} are shown. The indirect limits on d_A^g (neutron electric dipole moment) and on d_V^g (rare B meson decays) are presented as well as the limits from the combination of $t\bar{t}$ cross section at the LHC8 and Tevatron. Also, the limits which could be derived from tail of $t\bar{t}$ mass spectrum at the FCC-hh and LHC are shown.

while the ones from $t\bar{t}$ spectrum and the inclusive cross section at LHC14 with 100 fb^{-1} are $|d_A^g| \leq 0.019$ [9].

The combination of $t\bar{t}WW$ and $t\bar{t}ZZ$ channels provides the limits of $-0.007 \leq d_V^g \leq 0.008$ and $|d_A^g| \leq 0.007$ with an integrated luminosity of 3 ab^{-1}. The limits from $t\bar{t}WW$ (same-sign leptons), $t\bar{t}ZZ$ (four-lepton) and their combination are comparable to the limits from other studies and in some cases would be even better. The bounds obtained from this analysis could be improved by including the other signatures and taking into account the higher order QCD corrections in the signal channels. It should be indicated that while the indirect limits from the rare B decays and the neutron electric dipole moment are stronger but they are complementing each other.

Now, we turn to the weak dipole moments d_V^Z and d_A^Z. The expected constraints from an electron-positron collider at $\sqrt{s} = 500$ GeV with an integrated luminosity of 500 fb^{-1}, are $|d_V^Z| \leq 0.08$ and $-0.02 \leq d_A^Z \leq 0.04$ [27]. These limits are derived by exploiting the total cross section of the top quark pair production. The limits from the LHC top pair production at the center-of-mass energy of 14 TeV with an integrated luminosity of 3 ab^{-1} are $|d_{V,A}^Z| \leq 0.08$ [27]. They are obtained from the $p_{T,Z}$ distribution in $t\bar{t}Z$ production. The expected limits from the present study as shown in Table VI are comparable with the ones from ILC and LHC in $t\bar{t}Z$ channel. At the end, it should be mentioned that our bounds are purely based on statistical sensitivity calculations and no experimental effects, which would weaken them, are taken into account. However, the combination of different decay channels for each process and considering QCD higher order corrections would lead to have larger statistics and significant improvements.

IV. SUMMARY AND CONCLUSIONS

Rare SM processes involving multitop-quark and multigauge-boson final states at the LHC provide an exciting opportunity to search for new physics effects. To assess those effects, searches could be performed using the effective field theory approach which could affect both the total cross sections and the differential distributions. Particularly, the impacts would be expected to be significantly visible in processes containing heavy particles in their final states. In this paper, for the first time, we study the strong and weak electric ($d_A^{g,Z}$) and magnetic ($d_V^{g,Z}$) dipole moments of the top quark through the $t\bar{t}WW$ and $t\bar{t}ZZ$ channels at the LHC14. As the SM values for $d_V^{g,Z}$ and $d_A^{g,Z}$ are very small, in case of facing a situation with $d_{V,A}^{g,Z}$ large enough, $t\bar{t}WW$ and $t\bar{t}ZZ$ channels provide promising ways to observe the corresponding excess over the expectation of the SM.

Based on the top quarks, W bosons and Z bosons decays, various signatures are available from which we have concentrated on the much cleaner same-sign dilepton and four-lepton topologies for $t\bar{t}WW$ and $t\bar{t}ZZ$ channels, respectively. Therefore, we assume the signals considered here are adequately distinguishable from the SM backgrounds and a comprehensive study with including the backgrounds and detector effects are left for a future work. We find constraints of $-0.1 \leq d_V^Z \leq 0.09$, $|d_A^Z| \leq 0.1$ for the weak dipole moments and $-0.007 \leq d_V^g \leq 0.008$, $|d_A^g| \leq 0.007$ for the strong dipole moments using 3 ab^{-1} of the integrated luminosity of data. The results are comparable with the prospective ones reachable from $t\bar{t}$ and $t\bar{t}Z$ at the LHC. However, there are rooms for significant improvements of the bounds which could be achieved by including different topologies and by taking into account the higher order QCD corrections to signal processes.

ACKNOWLEDGMENTS

M. M. N. would like to thank the Iran National Science Foundation (INSF) for the financial support.

[1] M. Cristinziani and M. Mulders, Top-quark physics at the Large Hadron Collider, J. Phys. G **44**, 063001 (2017); A. Giammanco and R. Schwienhorst, Single top-quark production at the Tevatron and the LHC, arXiv:1710.10699; A. Giammanco, Single top quark production at the LHC, Rev. Phys. **1**, 1 (2016).

[2] W. Buchmuller and D. Wyler, Effective Lagrangian analysis of new interactions and flavor conservation, Nucl. Phys. **B268**, 621 (1986).

[3] J. A. Aguilar-Saavedra, A minimal set of top anomalous couplings, Nucl. Phys. **B812**, 181 (2009).

[4] B. Grzadkowski, M. Iskrzynski, M. Misiak, and J. Rosiek, Dimension-six terms in the standard model Lagrangian, J. High Energy Phys. 10 (2010) 085.

[5] C. Arzt, M. B. Einhorn, and J. Wudka, Patterns of deviation from the standard model, Nucl. Phys. **B433**, 41 (1995).

[6] R. Contino, A. Falkowski, F. Goertz, C. Grojean, and F. Riva, On the validity of the effective field theory approach to SM precision tests, J. High Energy Phys. 07 (2016) 144.

[7] D. Atwood, S. Bar-Shalom, G. Eilam, and A. Soni, *CP* violation in top physics, Phys. Rep. **347**, 1 (2001).

[8] K. Whisnant, B. L. Young, and X. Zhang, Unitarity and anomalous top quark Yukawa couplings, Phys. Rev. D **52**, 3115 (1995); K. Fuyuto, W. S. Hou, and E. Senaha, Electroweak baryogenesis via top transport, Phys. Lett. B **776**, 402 (2018); J. M. Cline, K. Kainulainen, and M. Trott, Electroweak baryogenesis in two Higgs doublet models and B meson anomalies, J. High Energy Phys. 11 (2011) 089;

M. Jiang, L. Bian, W. Huang, and J. Shu, Impact of a complex singlet: Electroweak baryogenesis and dark matter, Phys. Rev. D **93**, 065032 (2016); A. Kobakhidze, L. Wu, and J. Yue, Electroweak baryogenesis with anomalous Higgs couplings, J. High Energy Phys. 04 (2016) 011.

[9] J. A. Aguilar-Saavedra, B. Fuks, and M. L. Mangano, Pinning down top dipole moments with ultra-boosted tops, Phys. Rev. D **91**, 094021 (2015).

[10] W. Bernreuther, L. Chen, I. Garca, M. Perell, R. Poeschl, F. Richard, E. Ros, and M. Vos, *CP*-violating top quark couplings at future linear e^+e^- colliders, Eur. Phys. J. C **78**, 155 (2018).

[11] S. D. Rindani, P. Sharma, and A. W. Thomas, Polarization of top quark as a probe of its chromomagnetic and chromoelectric couplings in tW production at the Large Hadron Collider, J. High Energy Phys. 10 (2015) 180.

[12] Z. Hioki and K. Ohkuma, Latest constraint on nonstandard top-gluon couplings at hadron colliders and its future prospect, Phys. Rev. D **88**, 017503 (2013).

[13] S. S. Biswal, S. D. Rindani, and P. Sharma, Probing chromomagnetic and chromoelectric couplings of the top quark using its polarization in pair production at hadron colliders, Phys. Rev. D **88**, 074018 (2013).

[14] D. Choudhury and P. Saha, Higgs production as a probe of anomalous top couplings, J. High Energy Phys. 08 (2012) 144.

[15] Z. Hioki and K. Ohkuma, Optimal-observable analysis of possible non-standard top-quark couplings in $pp- > t\bar{t}X- > l^+X'$, Phys. Lett. B **716**, 310 (2012).

[16] W. Bernreuther, D. Heisler, and Z. G. Si, A set of top quark spin correlation and polarization observables for the LHC: Standard model predictions and new physics contributions, J. High Energy Phys. 12 (2015) 026.

[17] S. K. Gupta, A. S. Mete, and G. Valencia, *CP* violating anomalous top-quark couplings at the LHC, Phys. Rev. D **80**, 034013 (2009).

[18] H. Hesari and M. Mohammadi Najafabadi, Direct photon production as a probe of quarks chromoelectric and chromomagnetic dipole moments at the LHC, Phys. Rev. D **91**, 057502 (2015).

[19] S. Yaser Ayazi, H. Hesari, and M. Mohammadi Najafabadi, Probing the top quark chromoelectric and chromomagnetic dipole moments in single top tW-channel at the LHC, Phys. Lett. B **727**, 199 (2013).

[20] H. Hesari and M. Mohammadi Najafabadi, Probing the anomalous couplings of the top quark with gluon at the LHC and Tevatron, Mod. Phys. Lett. A **28**, 1350170 (2013).

[21] H. Khanpour, S. Khatibi, M. Khatiri Yanehsari, and M. Mohammadi Najafabadi, Single top quark production as a probe of anomalous $tq\gamma$ and tqZ couplings at the FCC-ee, Phys. Lett. B **775**, 25 (2017).

[22] S. M. Etesami, S. Khatibi, and M. Mohammadi Najafabadi, Measuring anomalous WW γ and t $\bar{\text{t}}\gamma$ couplings using top $+\gamma$ production at the LHC, Eur. Phys. J. C **76**, 533 (2016).

[23] S. Khatibi and M. Mohammadi Najafabadi, Exploring the anomalous Higgs-top couplings, Phys. Rev. D **90**, 074014 (2014).

[24] W. Bernreuther and Z. G. Si, Distributions and correlations for top quark pair production and decay at the Tevatron and LHC, Nucl. Phys. **B837**, 90 (2010).

[25] M. Schulze and Y. Soreq, Pinning down electroweak dipole operators of the top quark, Eur. Phys. J. C **76**, 466 (2016).

[26] R. Rontsch and M. Schulze, Constraining couplings of top quarks to the Z boson in $t\bar{t}$ + Z production at the LHC, J. High Energy Phys. 07 (2014) 091; Erratum, J. High Energy Phys. 09 (2015) 132(E).

[27] R. Rontsch and M. Schulze, Probing top-Z dipole moments at the LHC and ILC, J. High Energy Phys. 08 (2015) 044.

[28] S. Fayazbakhsh, S. T. Monfared, and M. Mohammadi Najafabadi, Top quark anomalous electromagnetic couplings in photon-photon scattering at the LHC, Phys. Rev. D **92**, 014006 (2015).

[29] J. F. Kamenik, J. Shu, and J. Zupan, Review of new physics effects in t-tbar production, Eur. Phys. J. C **72**, 2102 (2012).

[30] A. O. Bouzas and F. Larios, Probing tt? and ttZ couplings at the LHeC, Phys. Rev. D **88**, 094007 (2013).

[31] Q. H. Cao, C. R. Chen, F. Larios, and C.-P. Yuan, Anomalous gtt couplings in the littlest Higgs model with T-parity, Phys. Rev. D **79**, 015004 (2009).

[32] R. Gaitan, E. A. Garces, J. H. M. de Oca, and R. Martinez, Top quark chromoelectric and chromomagnetic dipole moments in a two Higgs doublet model with *CP* violation, Phys. Rev. D **92**, 094025 (2015).

[33] M. Casolino, T. Farooque, A. Juste, T. Liu, and M. Spannowsky, Probing a light *CP*-odd scalar in di-top-associated production at the LHC, Eur. Phys. J. C **75**, 498 (2015).

[34] C. Englert, F. Krauss, M. Spannowsky, and J. Thompson, Di-Higgs phenomenology in $t\bar{t}hh$: The forgotten channel, Phys. Lett. B **743**, 93 (2015).

[35] C. Englert and M. Spannowsky, Effective theories and measurements at colliders, Phys. Lett. B **740**, 8 (2015).

[36] C. Englert, D. Goncalves, and M. Spannowsky, Nonstandard top substructure, Phys. Rev. D **89**, 074038 (2014).

[37] C. Englert, A. Freitas, M. Spira, and P. M. Zerwas, Constraining the intrinsic structure of top-quarks, Phys. Lett. B **721**, 261 (2013).

[38] F. Larios, T. M. P. Tait, and C. P. Yuan, Anomalous $W^+W^-t\bar{t}$ couplings at the e^+e^- linear collider, Phys. Rev. D **57**, 3106 (1998).

[39] C. Englert and M. Russell, Top quark electroweak couplings at future lepton colliders, Eur. Phys. J. C **77**, 535 (2017).

[40] J. Chang, K. Cheung, J. S. Lee, and C. T. Lu, Probing the top-Yukawa coupling in associated Higgs production with a single top quark, J. High Energy Phys. 05 (2014) 062.

[41] K. m. Cheung, Probing the chromoelectric and chromomagnetic dipole moments of the top quark at hadronic colliders, Phys. Rev. D **53**, 3604 (1996).

[42] O. Bessidskaia Bylund, F. Maltoni, I. Tsinikos, E. Vryonidou, and C. Zhang, Probing top quark neutral couplings in the standard model effective field theory at NLO in QCD, J. High Energy Phys. 05 (2016) 052.

[43] C. Degrande, J. M. Gerard, C. Grojean, F. Maltoni, and G. Servant, Non-resonant new physics in top pair production at hadron colliders, J. High Energy Phys. 03 (2011) 125.

[44] D. Buarque Franzosi and C. Zhang, Probing the top-quark chromomagnetic dipole moment at next-to-leading order in QCD, Phys. Rev. D **91**, 114010 (2015).

[45] D. Barducci, M. Fabbrichesi, and A. Tonero, Constraints on top quark nonstandard interactions from Higgs and $t\bar{t}$ production cross sections, Phys. Rev. D **96**, 075022 (2017).
[46] F. Maltoni, E. Vryonidou, and C. Zhang, Higgs production in association with a top-antitop pair in the standard model effective field theory at NLO in QCD, J. High Energy Phys. 10 (2016) 123.
[47] C. Englert, L. Moore, K. Nordstrm, and M. Russell, Giving top quark effective operators a boost, Phys. Lett. B **763**, 9 (2016).
[48] Y. T. Chien, V. Cirigliano, W. Dekens, J. de Vries, and E. Mereghetti, Direct and indirect constraints on *CP*-violating Higgs-quark and Higgs-gluon interactions, J. High Energy Phys. 02 (2016) 011.
[49] C. Degrande, J. M. Gerard, C. Grojean, F. Maltoni, and G. Servant, Probing top-Higgs non-standard interactions at the LHC, J. High Energy Phys. 07 (2012) 036; Erratum, J. High Energy Phys. 03 (2013) 32.
[50] C. Zhang and S. Willenbrock, Effective-field-theory approach to top-quark production and decay, Phys. Rev. D **83**, 034006 (2011).
[51] D. Azevedo, A. Onofre, F. Filthaut, and R. Gonalo, *CP* tests of Higgs couplings in $t\bar{t}h$ semileptonic events at the LHC, arXiv:1711.05292.
[52] F. Dliot, R. Faria, M. C. N. Fiolhais, P. Lagarelhos, A. Onofre, C. M. Pease, and A. Vasconcelos, Global constraints on top quark anomalous couplings, Phys. Rev. D **97**, 013007 (2018).
[53] J. A. Aguilar-Saavedra, M. C. N. Fiolhais, and A. Onofre, Top effective operators at the ILC, J. High Energy Phys. 07 (2012) 180.
[54] M. Mohammadi Najafabadi, Probing of Wtb anomalous couplings via the tW channel of single top production, J. High Energy Phys. 03 (2008) 024.
[55] H. Hesari, H. Khanpour, and M. Mohammadi Najafabadi, Direct and indirect searches for top-Higgs FCNC couplings, Phys. Rev. D **92**, 113012 (2015).
[56] E. Boos, V. Bunichev, L. Dudko, and M. Perfilov, Modeling of anomalous Wtb interactions in single top quark events using subsidiary fields, Int. J. Mod. Phys. A **32**, 1750008 (2017).
[57] E. Boos and L. Dudko, The single top quark physics, Int. J. Mod. Phys. A **27**, 1230026 (2012).
[58] T. G. Rizzo, Single top quark production as a probe for anomalous moments at hadron colliders, Phys. Rev. D **53**, 6218 (1996).
[59] A. Buckley, C. Englert, J. Ferrando, D. J. Miller, L. Moore, M. Russell, and C. D. White, Constraining top quark effective theory in the LHC Run II era, J. High Energy Phys. 04 (2016) 015.
[60] A. Buckley, C. Englert, J. Ferrando, D. J. Miller, L. Moore, M. Russell, and C. D. White, Global fit of top quark effective theory to data, Phys. Rev. D **92**, 091501 (2015).
[61] K. Fuyuto and M. Ramsey-Musolf, Top down electroweak dipole operators, arXiv:1706.08548.
[62] P. Torrielli, Rare standard model processes for present and future hadronic colliders, arXiv:1407.1623.
[63] H. van Deurzen, R. Frederix, V. Hirschi, G. Luisoni, P. Mastrolia, and G. Ossola, Spin polarisation of $t\bar{t}\gamma\gamma$ production at NLO + PS with GoSam interfaced to MadGraph5aMC@NLO, Eur. Phys. J. C **76**, 221 (2016).
[64] E. Alvarez, D. A. Faroughy, J. F. Kamenik, R. Morales, and A. Szynkman, Four tops for LHC, Nucl. Phys. **B915**, 19 (2017).
[65] M. Aaboud *et al.* (ATLAS Collaboration), Measurement of the $t\bar{t}Z$ and $t\bar{t}W$ production cross sections in multilepton final states using 3.2 fb^{-1} of pp collisions at $\sqrt{s} = 13$ TeV with the ATLAS detector, Eur. Phys. J. C **77**, 40 (2017).
[66] A. M. Sirunyan *et al.* (CMS Collaboration), Measurement of the cross section for top quark pair production in association with a W or Z boson in proton-proton collisions at $\sqrt{s} = 13$ TeV, arXiv:1711.02547.
[67] R. Martinez and J. A. Rodriguez, The anomalous chromomagnetic dipole moment of the top quark in the standard model and beyond, Phys. Rev. D **65**, 057301 (2002).
[68] R. Martinez, M. A. Perez, and N. Poveda, Chromomagnetic dipole moment of the top quark revisited, Eur. Phys. J. C **53**, 221 (2008).
[69] CMS Collaboration, Report No. CMS-PAS-TOP-14-005.
[70] J. F. Kamenik, M. Papucci, and A. Weiler, Constraining the dipole moments of the top quark, Phys. Rev. D **85**, 071501 (2012); Erratum, Phys. Rev. D **88**, 039903 (2013).
[71] W. Hollik, J. I. Illana, S. Rigolin, C. Schappacher, and D. Stockinger, Top dipole form-factors and loop induced *CP* violation in supersymmetry, Nucl. Phys. **B551**, 3 (1999); Erratum,Nucl. Phys. **B557**, 407(E) (1999).
[72] J. Bernabeu, D. Comelli, L. Lavoura, and J. P. Silva, Weak magnetic dipole moments in two Higgs doublet models, Phys. Rev. D **53**, 5222 (1996).
[73] T. Ibrahim and P. Nath, The top quark electric dipole moment in an MSSM extension with vector like multiplets, Phys. Rev. D **82**, 055001 (2010).
[74] K. Agashe, G. Perez, and A. Soni, Collider signals of top quark flavor violation from a warped extra dimension, Phys. Rev. D **75**, 015002 (2007).
[75] C. Englert and M. Russell, Top quark electroweak couplings at future lepton colliders, Eur. Phys. J. C **77**, 535 (2017).
[76] J. Alwall *et al.*, The automated computation of tree-level and next-to-leading order differential cross sections, and their matching to parton shower simulations, J. High Energy Phys. 07 (2014) 079.
[77] R. D. Ball *et al.* (NNPDF Collaboration), Parton distributions for the LHC Run II, J. High Energy Phys. 04 (2015) 040.
[78] A. Alloul, N. D. Christensen, C. Degrande, C. Duhr, and B. Fuks, FeynRules 2.0—A complete toolbox for tree-level phenomenology, Comput. Phys. Commun. **185**, 2250 (2014).
[79] C. Degrande, C. Duhr, B. Fuks, D. Grellscheid, O. Mattelaer, and T. Reiter, UFO—The universal FeynRules output, Comput. Phys. Commun. **183**, 1201 (2012).
[80] T. Sjostrand, S. Mrenna, and P. Z. Skands, A brief introduction to PYTHIA 8.1, Comput. Phys. Commun. **178**, 852 (2008).
[81] M. Cacciari, G. P. Salam, and G. Soyez, The anti-k(t) jet clustering algorithm, J. High Energy Phys. 04 (2008) 063.
[82] J. de Favereau, C. Delaere, P. Demin, A. Giammanco, V. Lemaître, A. Mertens, and M. Selvaggi (DELPHES 3 Collaboration), DELPHES 3, A modular framework for

fast simulation of a generic collider experiment, J. High Energy Phys. 02 (2014) 057.

[83] S. Chatrchyan *et al.* (CMS Collaboration), The CMS Experiment at the CERN LHC, J. Instrum. **3**, S08004 (2008).

[84] F. Maltoni, D. Pagani, and I. Tsinikos, Associated production of a top-quark pair with vector bosons at NLO in QCD: impact on $t\bar{t}H$ searches at the LHC, J. High Energy Phys. 02 (2016) 113.

[85] B. Grzadkowski and M. Misiak, Anomalous Wtb coupling effects in the weak radiative B-meson decay, Phys. Rev. D **78**, 077501 (2008); Erratum, Phys. Rev. D **84**, 059903(E) (2011).

[86] C. Bernardo, N. F. Castro, M. C. N. Fiolhais, H. Gonalves, A. G. C. Guerra, M. Oliveira, and A. Onofre, Studying the *Wtb* vertex structure using recent LHC results, Phys. Rev. D **90**, 113007 (2014).